KfK 4245
Mai 1987

Analysis of Expansion Phase Experiments with Improved Approximation Schemes

J. J. Foit
Institut für Neutronenphysik und Reaktortechnik
Projekt Schneller Brüter

Kernforschungszentrum Karlsruhe

KERNFORSCHUNGSZENTRUM KARLSRUHE

Institut für Neutronenphysik und Reaktortechnik

Projekt Schneller Brüter

KfK 4245

Analysis of Expansion Phase Experiments with Improved Approximation Schemes

J.J. Foit

Kernforschungszentrum Karlsruhe GmbH, Karlsruhe

Kernforschungszentrum Karlsruhe GmbH
Postfach 3640, 7500 Karlsruhe 1

ISSN 0303-4003

Abstract

A steady-state flow of a single-phase and incompressible fluid across a singularity is studied. Based on these theoretical considerations new approximation methods for the pressure gradient term in the SIMMER-II momentum equations are proposed which give a satisfactory pressure change in flows across singularities.

The expansion phase experiments with a dipplate performed by SRI-International are evaluated to examine the quality of the proposed approximation schemes.

Analyse von Experimenten zur Expansionsphase mit verbesserten Approximations-Verfahren

Zusammenfassung

Es werden stationäre einphasige und inkompressible Strömungen durch abrupte Querschnittsänderungen untersucht. Anhand dieser theoretischen Untersuchungen werden geeignete Approximationsmethoden des Volumenanteiles im Druckgradiententerm in den SIMMER-II Impulsgleichungen angegeben, die zufriedenstellende Druckverläufe in Strömungen durch abrupte Querschnittsänderungen liefern.

Expansionsexperimente mit einer Tauchplatte, die bei SRI-International durchgeführt wurden, werden nachgerechnet, um die neuen Verfahren zu testen.

Introduction

The SIMMER-II discretization of the momentum equations is responsible for many problems encountered in calculations of flows through singularities. For example the equations violate the hydrostatic laws and yield too low mass flow rates in the presence of area changes. This insufficiency of the SIMMER-II code was observed in former SIMMER-II calculations of the SNR-type Expansion Phase Experiments with a perforated dipplate. In order to circumvent these difficulties the area ratio of the dipplate had to be artificially increased /5/.

In order to set up an improved form of the momentum difference equations, which give a good representation of the flow across abrupt area changes, the steady-state flow of a single-phase and incompressible fluid is studied.

In the first part of this report new approximation schemes are proposed and compared with the momentum equations used in the original SIMMER-II code.

In the second part of this paper the experiments performed by SRI-International in close cooperation with the Nuclear Research Center Karlsruhe are evaluated using the corrected and the original SIMMER-II.10 code, and those calculational results are compared with the experimental data. This series of experiments was performed in order to simulate the post-disassembly expansion phase in a 1/20-scale model of the SNR-300 reactor vessel and to obtain data for the test and the validation of the SIMMER-II code.

It is demonstrated that the improved formulation of the momentum difference equation gives a much better agreement with the experiments without the necessity to increase the area ratio of the dipplate in an artificial way as in /5/.

1. Flow through sudden expansions and contractions

1.1 General considerations for sudden expansions and contractions

In this chapter the behaviour of the steady-state flow of a single-phase and incompressible fluid across a singularity is analyzed.

1.1.1 Sudden expansion

First we want to calculate the pressure change caused by a sudden expansion shown in Fig. 1.

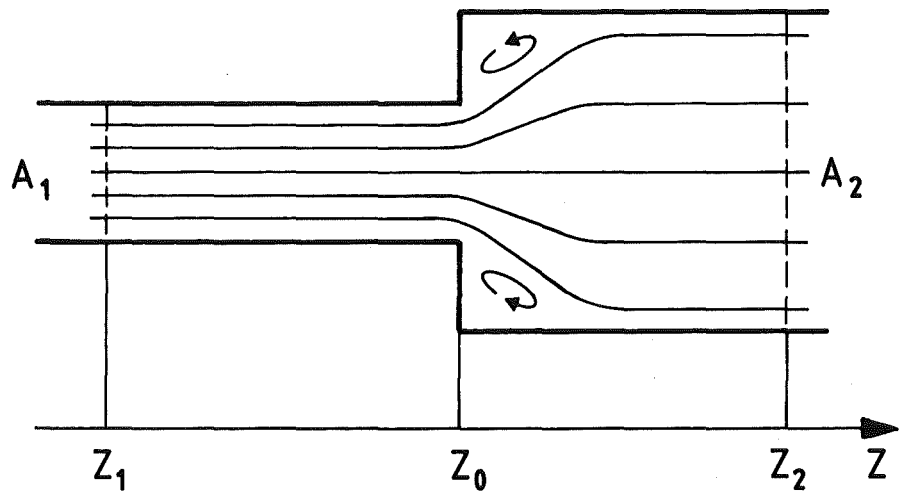

Fig. 1. Sudden expansion

In the following the viscous effects are assumed to be negligible. In this case the momentum equation has the form

$$\int_{z_1}^{z_2} \partial_z(A(z)\rho\langle v^2\rangle)dz + \int_{z_1}^{z_2} A(z)\partial_z\langle p\rangle dz = 0 \qquad (1)$$

where
$\langle f\rangle = \frac{1}{A}\int_A f dA$ is the area-averaged quantity f,

v is the velocity,
ρ the microscopic density and
p is the pressure.

The cross-section in Fig. 1 can be written as

$$A(z) = A_1 + (A_2-A_1)\theta(z-z_0) \tag{2}$$

with

$$\theta(z-z_0) = \begin{cases} 0 \text{ for } z \leq z_0 \\ 1 \text{ for } z > z_0 \end{cases} \tag{3}$$

Integration by parts of the second term of Eq. (1) leads to the following expression:

$$\int_{z_1}^{z_2} A(z)\partial_z <p> dz = <p> \left[A_1 + (A_2-A_1)\theta(z-z_0)\right] \Big|_{z_1}^{z_2}$$

$$-\int_{z_1}^{z_2} <p>(A_2-A_1)\delta(z-z_0)dz = A_2 <p>_2 - A_1 <p>_1 - <p>_0(A_2-A_1). \tag{4}$$

In order to derive an expression for the pressure difference

$$\Delta p: = <p>_1 - <p>_2 \tag{5}$$

from equation (4) we have to make an assumption about the pressure at the point z_0. It is reasonable to make the approximation (see for example /2/)

$$<p>_0 = <p>_1 \tag{6}$$

Consequently, we obtain from equations (1), (4) and (6)

$$\Delta p = \rho \left[<v^2>_2 - <v^2>_1 A_1/A_2\right] . \tag{7}$$

For the example considered mass conservation yields

$$<v>_2 = \tau <v>_1 \tag{8}$$

where

$$\tau = A_1/A_2 \tag{9}$$

If we assume that the velocity profile is flat, we have

$$<v^2> = <v>^2 \tag{10}$$

and finally we obtain from equations (7) - (10)

$$\Delta p = \rho <v>_1^2 \tau(\tau\text{-}1) . \tag{11}$$

Applying the Bernoulli equation along the streamline between points z_1 and z_2 we have

$$\Delta p = \tfrac{1}{2} \rho <v>_1^2 (\tau^2\text{-}1) . \tag{12}$$

This equation describes the reversible pressure increase in a sudden expansion.

The following table (Tab. 1) shows the data for the relative pressure rise ζ at a sudden expansion obtained from experiment /1/ and those calculated from equations (11) and (12):

τ	ζ_{exp}	ζ_{mom}	ζ_{Ber}
0.71	-0.33	-0.41	-0.49
0.48	-0.42	-0.499	-0.77
0.348	-0.45	-0.45	-0.88
0.155	-0.24	-0.26	-0.98
0.108	-0.18	-0.19	-0.99

Tab. 1. Comparison of calculated and measured pressure rise

where

$$\zeta_{mom} := \frac{\Delta p}{\tfrac{1}{2}\rho <v>_1^2} = 2\tau(\tau\text{-}1), \tag{13}$$

$$\zeta_{Ber} := \frac{\Delta p}{\tfrac{1}{2} \rho <v>_1^2} = \tau^2\text{-}1. \tag{14}$$

This comparison shows that the pressure change calculated from the momentum equation agrees very well with the experimental data. This fact justifies the assumption (6). For $\tau \to 0$ the results obtained by the Bernoulli equation become worse.

1.1.2 Sudden contraction

Let us now consider a sudden contraction as shown in Fig. 2.

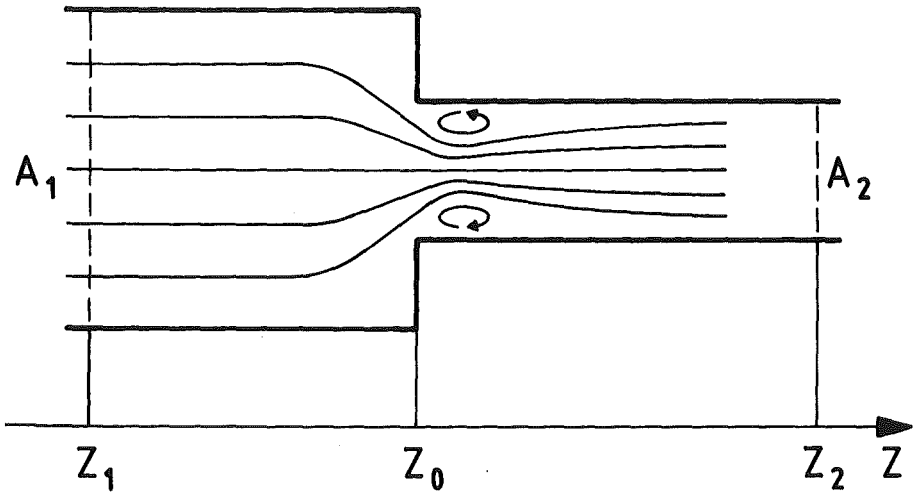

Fig. 2. Sudden contraction

In order to derive a formula for the pressure drop from the momentum equation, Eq. (1), we have to make an assumption about the pressure at the point z_0. As stated in /2/ we set

$$\langle p \rangle_0 = \langle p \rangle_1. \tag{15}$$

This approximation leads to

$$\eta_{mom} := \frac{\Delta p}{\frac{1}{2}\ \rho <v>_2^2} = 2(1 - 1/\tau). \tag{16}$$

On the other hand the Bernoulli equation gives the following expression

$$\eta_{Ber} := \frac{\Delta p}{\frac{1}{2}\ \rho <v>_2^2} = 1 - 1/\tau^2 . \tag{17}$$

The comparison with the experimental data /3/ given in Table 2 shows that the approximation (15) is not very good, especially for $1/\tau \to 0$, and that

$$<p>_0 < <p>_1. \tag{18}$$

$1/\tau$	η_{exp}	η_{mom}	η_{Ber}
0.828	0.35	0.34	0.31
0.504	0.98	0.99	0.75
0.25	1.3	1.5	0.94
0.1089	1.41	1.78	0.99
0.04	1.45	1.92	1.0
0.01	1.46	1.98	1.0
0	1.47	2.0	1.0

Tab. 2. Comparison of calculated and measured pressure drop

1.2 Difference equations of the pressure changes for sudden expansions and contractions

In this section expressions for the pressure difference of singularities are derived.

Let us consider a steady-state flow through the following (Fig. 3) area change.

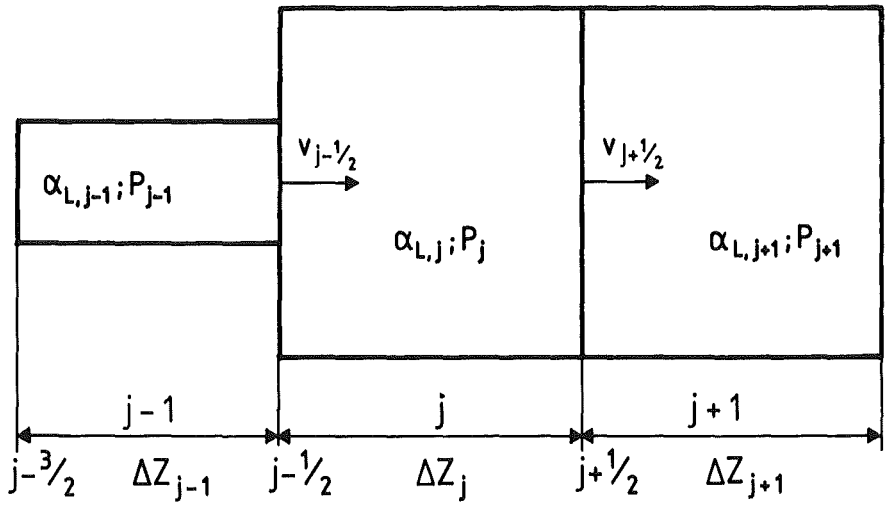

Fig. 3. Grid for a sudden expansion

The variable cross-sectional area is replaced by the liquid volume fraction α_L.

The formalism used in /4/ leads to the following momentum and continuity difference equations.

$$<\bar{\rho}v^2>_{j+1} - <\bar{\rho}v^2>_j + \tilde{\alpha}_{L,j+1/2} \quad (p_{j+1} - p_j) = 0, \tag{19}$$

$$<\bar{\rho}v>_{j+1/2} - <\bar{\rho}v>_{j-1/2} = 0 \tag{20}$$

where we have

$$\bar{\rho} = \rho\alpha_L \text{ and} \tag{21}$$

$$<\bar{\rho}v^2>_j := v_j \tfrac{1}{2} \left[(1+\mathrm{sgn}v_j)(\bar{\rho}v)_{j-1/2} + (1-\mathrm{sgn}v_j)(\bar{\rho}v)_{j+1/2} \right], \tag{22}$$

$$<\bar{\rho}v>_{j+1/2} := v_{j+1/2} \cdot \tfrac{1}{2} \left[(1+\mathrm{sgn}v_{j+1/2})\,\bar{\rho}_j + (1-\mathrm{sgn}v_{j+1/2})\,\bar{\rho}_{j+1} \right] \tag{23}$$

and

$$(\bar{\rho}v)_j := \bar{\rho}_j v_j \tag{24}$$

For the sake of simplicity, we want to consider a uniform grid, i.e. $\Delta z_j = \Delta z_{j+1}$ for all j. In this case we have

$$v_j := \tfrac{1}{2}(v_{j+1/2} + v_{j-1/2}) \text{ and} \tag{25}$$

$$\bar{\rho}_{j+1/2} := \tfrac{1}{2}(\bar{\rho}_{j+1} + \bar{\rho}_j) = \tfrac{1}{2}\rho(a_{L,j+1} + a_{L,j}). \tag{26}$$

Additionally, we assume that

$$v_{j+1/2} > 0 \quad \text{for all} \quad j. \tag{27}$$

After some algebra we get from equations (19) - (27)

$$\Delta p_j = 1/2\ \rho v^2_{j-1/2}\ \zeta_j(\tilde{a}_{L,j-1/2}) \tag{28}$$

and

$$\Delta p_{j+1} = \tfrac{1}{2}\rho v^2_{j-1/2}\ \zeta_{j+1}(\tilde{a}_{L,j-1/2}) \tag{29}$$

where

$$\Delta p_j := p_{j-1} - p_j, \tag{30}$$

$$\Delta p_{j+1} := p_{j-1} - p_{j+1}, \tag{31}$$

$$\zeta_j(\tilde{a}_{L,j-1/2}) = \tfrac{1}{2}\ \frac{a_{L,j} + a_{L,j-1}}{a_{L,j-1/2}}\ (1+\tau) - 2\ \frac{a_{L,j-1}}{a_{L,j-1/2}} \tag{32}$$

and

$$\zeta_{j+1}(\tilde{a}_{L,j-1/2}) = \zeta_j(\tilde{a}_{L,j-1/2}) + 2\tau^2 - \tfrac{1}{2}(1+\tau)^2, \tag{33}$$

and τ denotes

$$\tau := \frac{a_{L,j-1}}{a_{L,j}}\ . \tag{34}$$

From equations (32) and (33) we deduce:

1. for a sudden expansion $\tau<1$ there is

$$p_{j+1} > p_j;$$

2. for a sudden contraction $\tau>1$

$$p_{j+1} < p_j;$$

3. the calculated pressure difference depends on the approximation of $\alpha_{L,j-1/2}$ which is equivalent to the assumption about the pressure at the point j-1/2 as it can be shown from Eq. (4).

In the case of the sudden expansion Fig. 3, equation (15) implies

$$p_{j-1/2} = p_{j-1} \tag{35}$$

and we have

$$\tilde{\alpha}_{L,j-1/2} = \alpha_{L,j} = \max(\alpha_{L,j-1}, \alpha_{L,j}). \tag{36}$$

Substitution of Eq. (36) into Eq. (32) and Eq. (33) gives

$$\zeta_j(\alpha_{L,j}) = \tfrac{1}{2}(\tau-1)^2 \tag{37}$$

and

$$\zeta_{j+1}(\alpha_{L,j}) = 2\tau(\tau-1). \tag{38}$$

The pressure change Δp_{j+1} (Eq. (29)) calculated from the difference momentum equation, Eq. (19) and Eq. (36), is exactly the same as the one derived theoretically in Eq. (11). Because of

$$\zeta_j(\alpha_{L,j}) > 0 \tag{39}$$

we get a pressure drop $p_j < p_{j-1}$ instead of a pressure rise.

In the SIMMER-II code the approximation

$$\tilde{a}_{L,j-1/2} = \min (a_{L,j-1}, a_{L,j}) = a_{L,j-1} \tag{40}$$

is used which is equivalent to the assumption $p_{j-1/2} = p_j$ and we obtain

$$\zeta_j(a_{L,j-1}) = \frac{(\tau-1)^2}{2\tau} \tag{41}$$

$$\zeta_{j+1}(a_{L,j-1}) = (\tau^2-1)\frac{3\tau-1}{2\tau} \tag{42}$$

Finally the approximation consistent with the averaging of the densities Eq. (26) is considered, i.e.

$$\tilde{a}_{L,j-1/2} = a_L^A := \tfrac{1}{2}(a_{L,j-1} + a_{L,j}). \tag{43}$$

This approximation implies that the difference momentum equation does not violate the hydrostatic law in the presence of area changes which is the case for the other approximations considered. The functions ζ are given by

$$\zeta_j(a_L^A) = \frac{(\tau-1)^2}{\tau+1}, \tag{44}$$

$$\zeta_{j+1}(a_L^A) = \tfrac{1}{2}\frac{\tau-1}{\tau+1}\,(3\tau^2+6\tau-1)\,. \tag{45}$$

Let us now consider a sudden contraction as shown in Fig. 4, i.e. $\tau > 1$. The pressure drop is scaled with the downstream kinetic energy, i.e.

$$\Delta p_j = \tfrac{1}{2}\rho v^2_{j+1/2} \cdot \eta_j(\tilde{a}_{L,j-1/2}) \tag{46}$$

and

$$\Delta p_{j+1} = \tfrac{1}{2}\rho v^2_{j+1/2} \cdot \eta_{j+1}(\tilde{\alpha}_{L,j-1/2}). \tag{47}$$

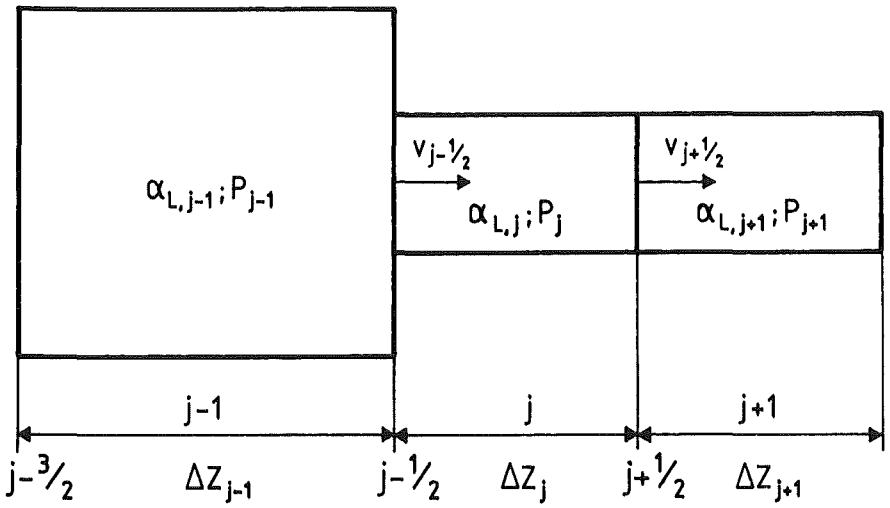

Fig. 4. Grid for a sudden contraction

It is easy to calculate the functions η from ζ using the equation of mass conservation, Eq. (20). Consequently we have

$$\eta_j(\alpha_{L,j}) = \tfrac{1}{2}(1-1/\tau)^2, \tag{48}$$

$$\eta_{j+1}(\alpha_{L,j}) = 2\,(1-1/\tau), \tag{49}$$

for the assumption

$$p_{j-1/2} = p_{j-1}$$

or, equivalently,

$$\tilde{\alpha}_{L,j-1} = \min(\alpha_{L,j-1},\alpha_{L,j}) = \alpha_{L,j}. \tag{50}$$

As mentioned above SIMMER-II makes use of approximation (50).

For $p_{j-1/2} = p_j$, i.e.: $\tilde{\alpha}_{L,j-1/2} = \max(\alpha_{L,j-1}, \alpha_{L,j}) = \alpha_{L,j-1}$,

we obtain

$$\eta_j(\alpha_{L,j-1}) = \tfrac{1}{2}\, 1/\tau\, (1-1/\tau)^2 \tag{51}$$

and

$$\eta_{j+1}(\alpha_{L,j-1}) = \tfrac{1}{2}\,(1-1/\tau^2)\,(3-1/\tau). \tag{52}$$

The averaging method (43) implies

$$\eta_j(\alpha_L^A) = 1/\tau \frac{1-1/\tau}{1+1/\tau}\quad , \tag{53}$$

$$\eta_{j+1}(\alpha_L^A) = \frac{1-1/\tau}{2\,(1\,+\,1/\tau\,)}\,(6/\tau - 1/\tau^2 + 3)\,. \tag{54}$$

1.3 Discussion of the results for the pressure changes in sudden expansions and contractions

The subsequent figures show the results for the pressure difference obtained by the analytical solution of the momentum and energy equations (Section 1.1) and the pressure difference calculated from the difference momentum equation (Section 1.2). The pressure loss coefficient related to the second mesh of a sudden expansion (Fig. 3) for various approximations of the volume fraction in the pressure gradient term is depicted in Fig. 5.

All approximations different from Eq. (36) lead to a pressure drop for $\tau < \tau_{kr}$ instead of a pressure rise. The approximations (36) reproduces the analytical solution of the momentum equation. Tab. 1 shows that the agreement between this analytical solution and the experiment is reasonably good.

In the first mesh of a sudden expansion (Fig. 6) a pressure drop instead of a pressure rise is obtained for all approximations of α. The SIMMER-II approximation becomes progessively worse as $\tau \to 0$.

In the case of a sudden contraction Fig. 4 the results of a pressure loss coefficient related to the second mesh are shown in Fig. 7. The approximation (40) used in

SIMMER-II leads to the same pressure drop as given by theoretical considerations (Eq. (16)). The assumption

$$p_{j-1/2} = p_{j-1}$$

which leads to the approximation considered is not satisfactory. The theoretical values of the pressure change are overestimated in comparison with the experiment. The best agreement with the experimental data is achieved by the approximation (36) and (43).

The pressure loss coefficient related to the first mesh (Fig. 8) is too small for all the approximations considered. The averaging method and the approximation (36) give a vanishing pressure difference for small $1/\tau$.

In those cases where the effect of the hydrostatic pressure is negligible the approximation given in Eq. (36) yields the best results and should therefore be used. The approximation (43) should be preferred if the hydrostatic effects dominate.

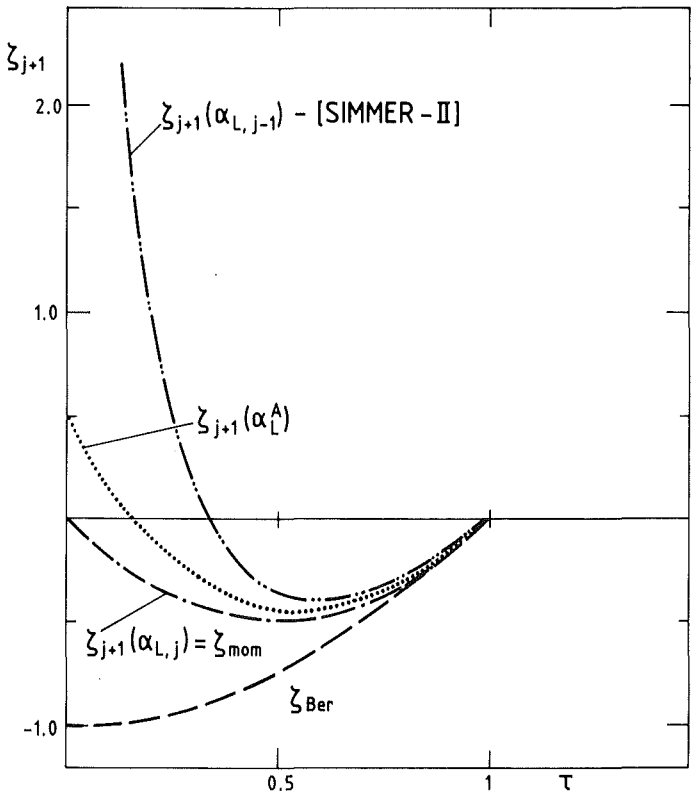

Fig. 5. Pressure loss coefficient ζ_{j+1}

$\zeta_{j+1}(\alpha_L^A)$ corresponds to the averaging method (Eq. 43);

$\zeta_{j+1}(\alpha_{L,j})$ corresponds to Eq. (36);

ζ_{mom} corresponds to the analytical solution (Eq. 13).

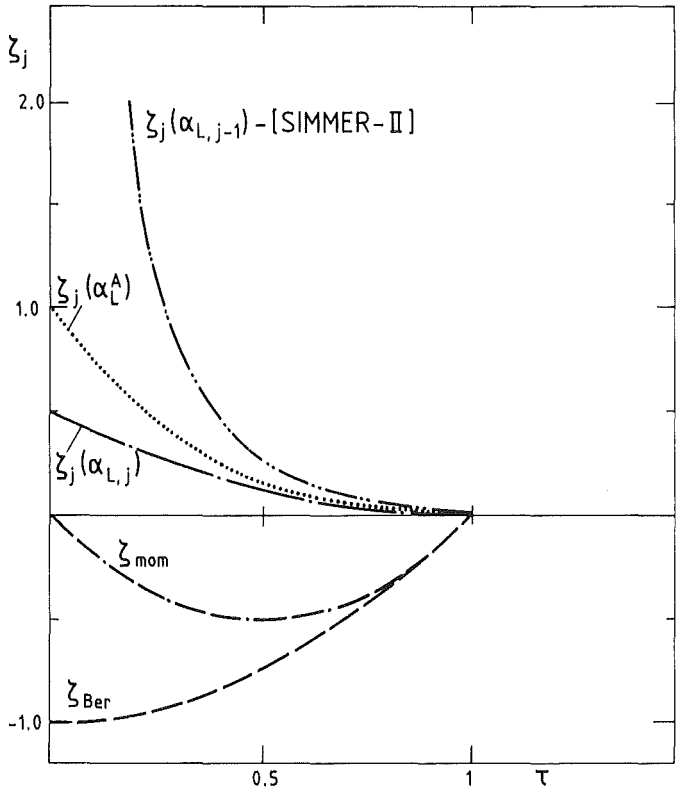

Fig. 6. Pressure loss coefficient ζ_j

$\zeta_j(a_L^A)$ corresponds to the averaging method (Eq. 43);

$\zeta_j(a_{L,j})$ corresponds to Eq. (36);

ζ_{mom} corresponds to the analytical solution (Eq. 13).

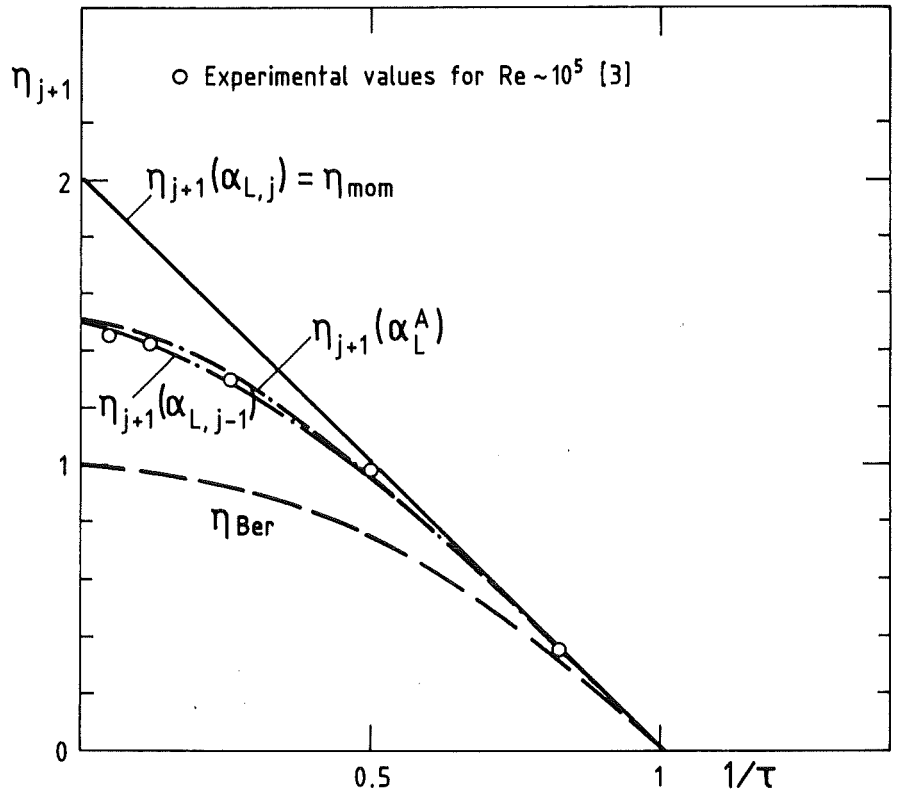

Fig. 7. Pressure loss coefficient η_{j+1}

$\eta_{j+1}(\alpha_L^A)$ corresponds to the averaging method (Eq. 43);

$\eta_{j+1}(\alpha_{L,j-1})$ corresponds to Eq. (36);

$\eta_{j+1}(\alpha_{L,j})$ corresponds to the SIMMER-II solution.

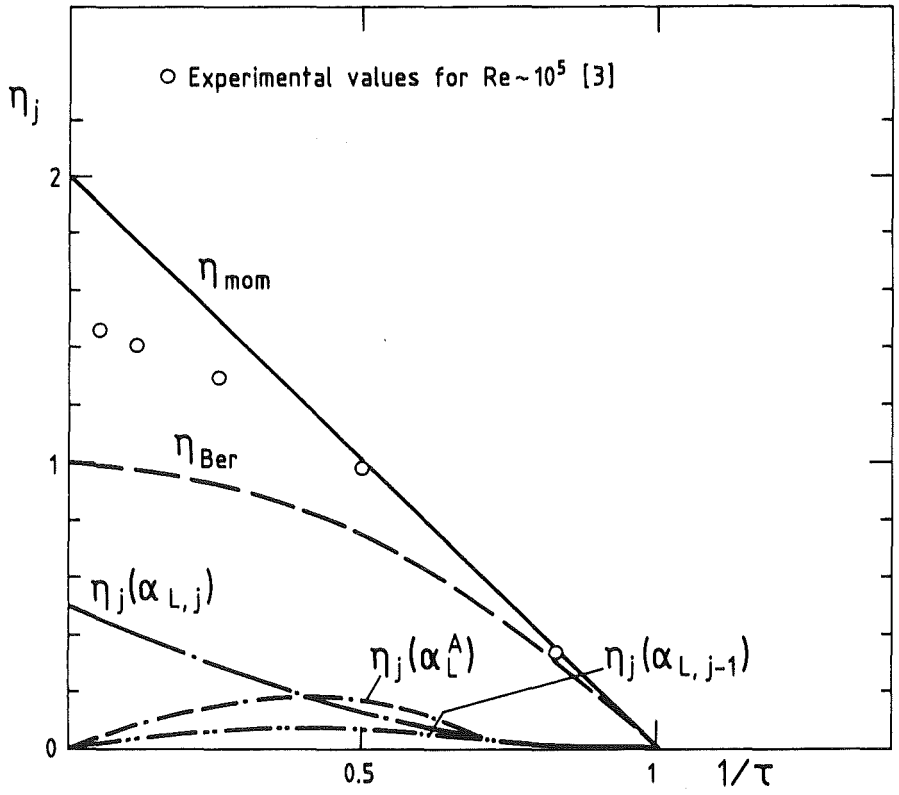

Fig. 8. Pressure loss coefficient η_j in the first mesh of a sudden contraction

$\eta_j(\alpha_L^A)$ corresponds to the averaging method (Eq. 43);

$\eta_j(\alpha_{L,j-1})$ corresponds to Eq. (36);

η_{mom} corresponds to the analytical solution (Eq. 16);

$\eta_j(\alpha_{L,j})$ corresponds to the SIMMER-II solution.

2. Analysis of the post-disassembly expansion phase experiments

2.1 Description of the SRI-experiments

In order to simulate the post-disassembly expansion phase in a 1/20-scale model of the SNR-300 reactor vessel a series of experiments were performed by SRI-International /6/ in close cooperation with KfK. The purpose of this experimental program was to study the physical phenomena and to obtain data for the test and the validation of the SIMMER-II code. A detailed description of these experiments as well as an analysis of the SIMMER-II.9 computational results are given in /5/. The basic model with a dipplate is shown in Fig. 9.

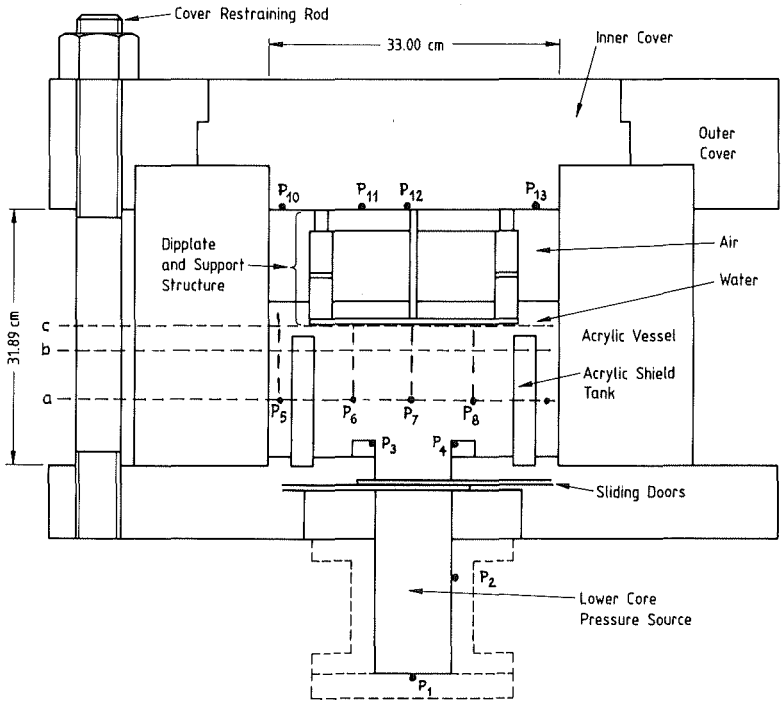

Fig. 9. Geometry of the 1/20-scale model

The internal structures and pressure sources used in experiments SNR05 through SNR08, which are considered in this paper, are shown in the following table (Tab. 3). Experiments SNR06 and SNR08 are repeats of experiments SNR05 and SNR07.

Experiment number	Upper core structure structure	Upper Internal	Dipplate (% open) (MPa)	Initial pressure
SNR05	No	No	Yes (20)	2.14
SNR06	No	No	Yes (20)	2.14
SNR07	No	No	Yes (20)	10.0
SNR08	No	No	Yes (20)	10.0

Tab. 3. Matrix of the experiments

The dipplate with a nominal porosity of 20% consists of 966 flow holes with a diameter of 0.345 cm. The virtual area ratio of this perforated plate is equal to 32% (see /6/).

Both nitrogen pressure sources 2.14 MPa and 10 MPa with volumes 732 cm^3 and 11,307 cm^3, resp., have different pressure decay characteristics. The 2.14 MPa source simulates a slow pressure decrease and the 10 MPa pressure source a strong decay of pressure during the expansion. It is worth mentioning that the adiabatic expansion work of both pressure sources to the gas volume of the vessel (8000 cm^3) is the same, i.e. 11.49 kJ.

2.2 Computational model of the experimental set-up

All calculations are performed with the version 10 of the SIMMER-II code. This means that the input data set used in /5/ for version 9 has to be adapted properly. The two-dimensional cylindrical geometry with azimutal symmetry is used to model the experimental set-up (Fig. 10).

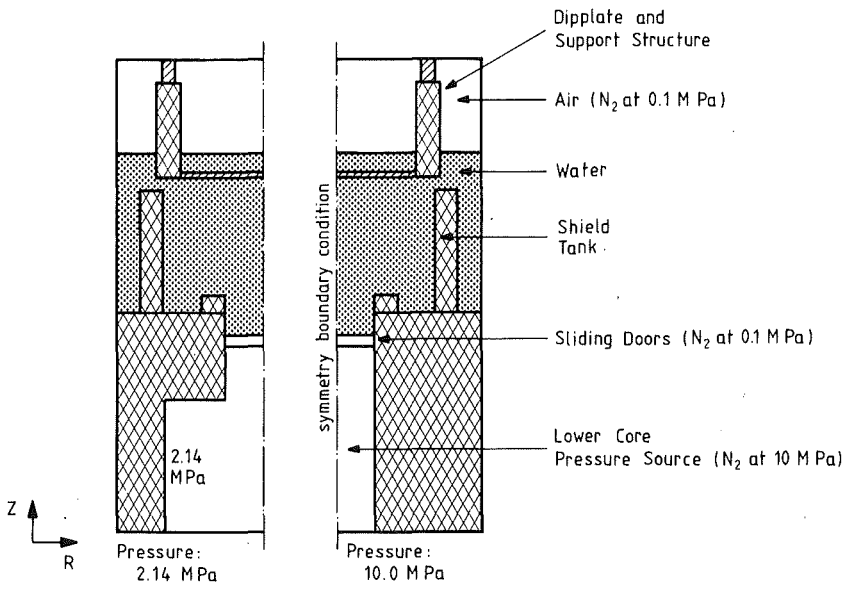

Fig. 10. Calculation model of the experimental apparatus

The neighbourhood of the dipplate is represented by a non-uniform grid. In the region just below (above) the perforated plate the grid step size varies by a factor 2.4 (2.8). This rather large changes in the grid step size can cause an unacceptable discretization error in the important flow regime where pressure changes across the singularities are calculated. In order to avoid this error the non-uniform part of the original grid is replaced by a uniform grid. The transition from this uniform subgrid to the coarser part of the calculation grid is achieved far away from the region of interest with a maximal change in the step size by a factor 1.8 (see Appendix 1).

2.3 Model of the dipplate

The theoretical results presented in the previous sections show why the porosity of the dipplate had to be increased in order to give correct mass flow rates in the original SIMMER-II calculations. In order to emphasize this point, the pressure loss coefficient ζ for a perforated plate with porosity τ_p is derived in the following using the results of section 1.2.

The SIMMER-II momentum equations lead to the following expression for ζ

$$\zeta_{SIM} = \frac{1-\tau_p}{2\tau_p^3} (-3\tau_p^2 + 2\tau_p + 1) \qquad (55)$$

which is easily obtained from Eq. (42) and Eq. (49).

For the approximation (43) (averaging of the volume fractions in the pressure gradient term) we get from Eq. (45) and Eq. (54)

$$\zeta_A = \frac{2}{\tau_p^2} (1-\tau_p)^2 . \qquad (56)$$

Finally for the approximation given in Eq. (36), we obtain from Eq. (38) and Eq. (52)

$$\zeta_{Max} = \frac{1-\tau_p}{2\tau_p^2} (-\tau_p^2 - 2\tau_p + 3). \qquad (57)$$

For the dipplate with the virtual porosity $\tau_p = 0.32$ as used in the experiments SNR05 through SNR08 the pressure loss coefficients are given in Tab. 4 for the various approximation schemes.

τ_p	ζ_{SIM}	ζ_A	ζ_{Max}
0.32	13.8	9.0	7.5

Tab. 4. Calculated pressure loss coefficients

Idelchik /7/ gives $\zeta = 9.9$ for the perforated thick plate of the experiments. The arguments given above justify the hope that the improved momentum equations will yield a good agreement between the experimental data and the computational results without increasing the porosity as it is necessary in calculations with the original SIMMER-II version in order to decrease the resistance coefficient.

3. Computational Results

3.1 General considerations

In the previous sections two approximation schemes to improve the modelling of the flow across singularities, i.e. abrupt area ratio changes, have been discussed. The approximation given in Eq. (36) leads to the best results for the pressure rise in a sudden expansion of the steady-state flow of a single-phase and incompressible fluid. The disadvantage of this method is a violation of the hydrostatic laws. If this scheme is implemented in the SIMMER-II code which is designed for two-phase flow, Eq. (36) cannot be fulfilled for both phases simultanously. The second approximation scheme described by Eq. (43) removes all these disadvantages but it doesn't give such a good representation of the pressure in a sudden expansion. Because of the fact that the approximation (43) treats both phases symmetrically, which is important for the two-phase flow and the conservation of the hydrostatic laws, this approximation scheme is preferable for our purpose. The experiments SNR05-SNR06 are calculated with both approximation methods, whereas the experiments SNR07-SNR08 are only analysed with the approximation described by Eq. (43). Additionally, the SNR05-SNR06 experiments are calculated with a coarser subgrid in the region below the dipplate. For all calculations which were performed in this report with the original SIMMER code, the actual value of the porosity was used in contrast to /5/ where the porosity had to be artificially increased in order to get a satisfactory agreement with the experimental results.

3.2 Impact times and pressure

The time of impact for the experiments 6 and 8 is determined by the pressure peaks of the pressure curves Fig. 11-14 for the central transducer (P12 in Fig. 9). The results for the experiments and calculations are given in the following table (Tab. 5).

Version of approximation	Calculation of SNR05-SNR06	Calculation of SNR07-SNR08	Measurement SNR06	Measurement SNR08
	Impact time (ms) / Impact pressure (MPa)			
SIMMER-II	7.44 / 4.5	4.51 / 3.62	6.58	3.86
Averaging: based on Eq. (43)	7.06 / 5.76	4.20 / 4.47		
Maximum: based on Eq. (36)	6.9 / 6.42	- / -	9.6	20

Tab. 5. Impact times and pressures

Pressure measurements were claimed /6/ to be accurate within $\pm 3\%$ for the maximum values. The errors obtained considering repeatability* were considerably higher ($\pm$ 13%). Impact times were resolved to 0.01 ms.

*Repeatibility was defined as the relative deviation of variables in trial and repeat. For experiments 5&6 no such comparison was possible because the top pressure transducers were not mounted in 5.

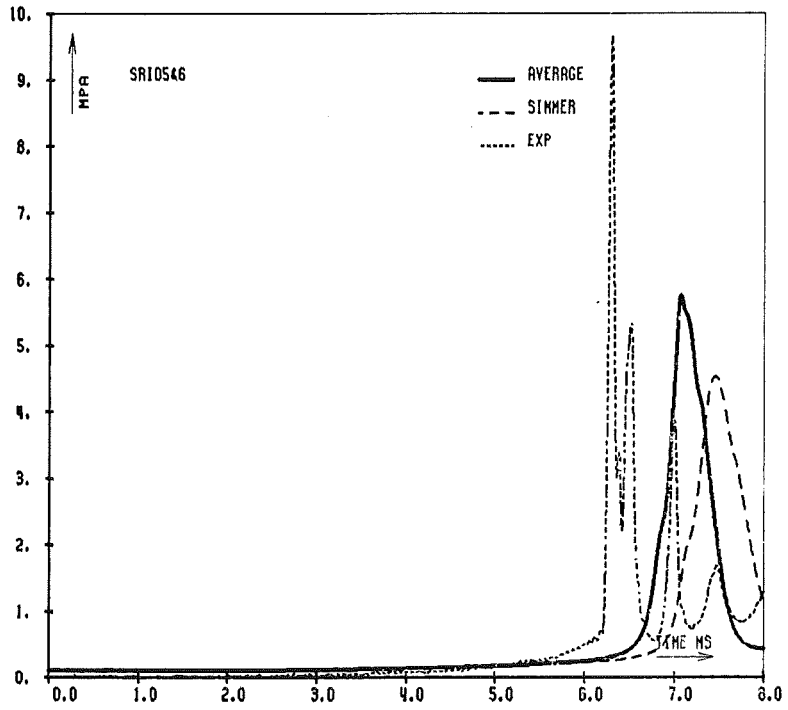

Fig. 11. Pressure at position P12 (see Fig. 9)

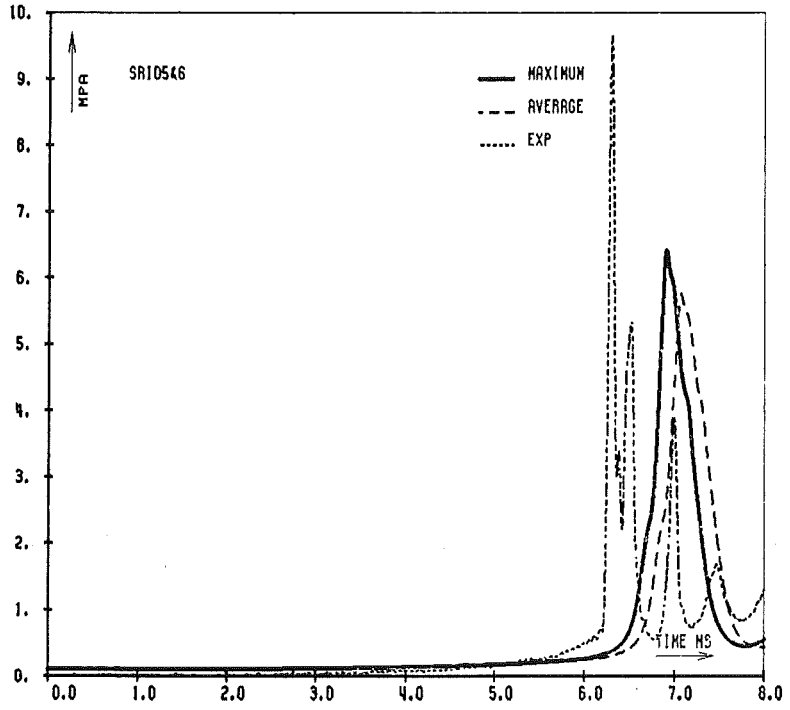

Fig. 12. Pressure at position P12 (see Fig. 9)

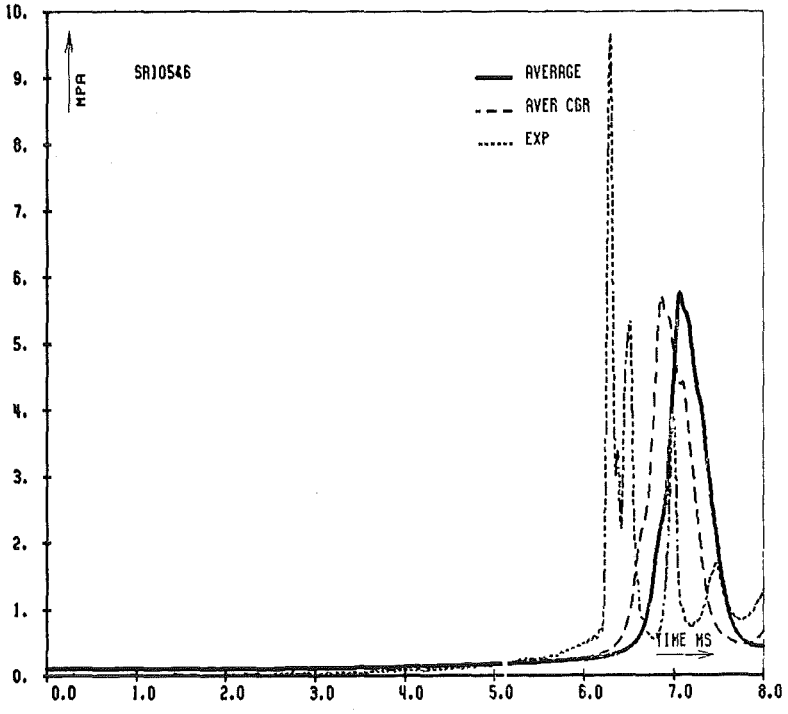

Fig. 13. Pressure at position P12 (CGR-result for the coarser subgrid)

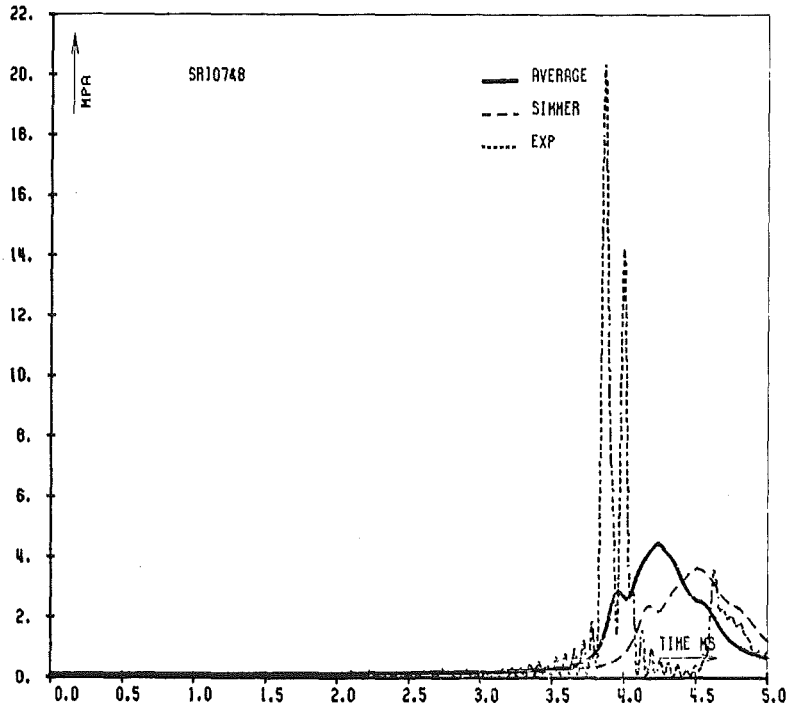

Fig. 14. Pressure at position P12

For the SNR05-SNR06 experiments the calculated amplitudes of the pressure peaks at the slug impact are lower than those obtained by the measurements. The results determined with the approximation scheme based on Eq. (43) are lower by a factor of 1.6. The factor 1.5 follows from the approximation (36). SIMMER-II leads to a pressure peak which is even 2.1 times lower. The calculated impact times show some delay in comparison with the experimental data: about 7% for the approximation schemes considered and 11% for the original SIMMER-II results. As it is shown in Fig. 13 the time of slug impact depends strongly on the grid. The coarse subgrid below the dipplate, as used in former calculations /5/, yielded an earlier slug impact than the measurement. The pressure peak is smeared out to a wide time interval. This fact caused a much lower impact pressure amplitude (factor 5) than measured.

The pressure at the central position P1 in the pressure source, which describes the decay characteristics of the pressure source, is well reproduced as it is shown in Fig. 15-16. The reason for the lower initial pressure (about 9 MPa instead of 10 MPa) for the high pressure source is that some gas was leaking out before the sliding doors were opened. SIMMER-II and the improved momentum equations lead to nearly the same results.

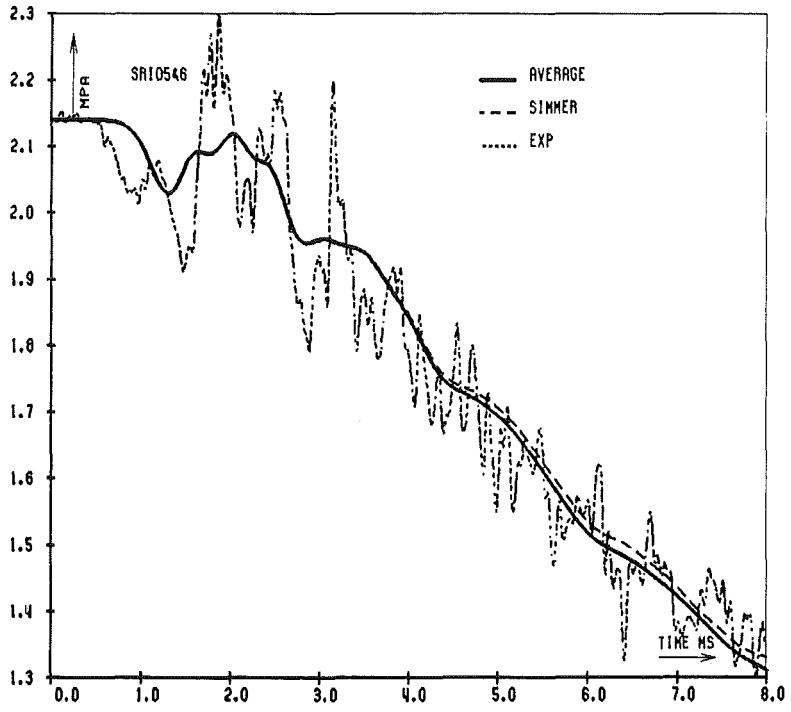

Fig. 15. Pressure at position P1

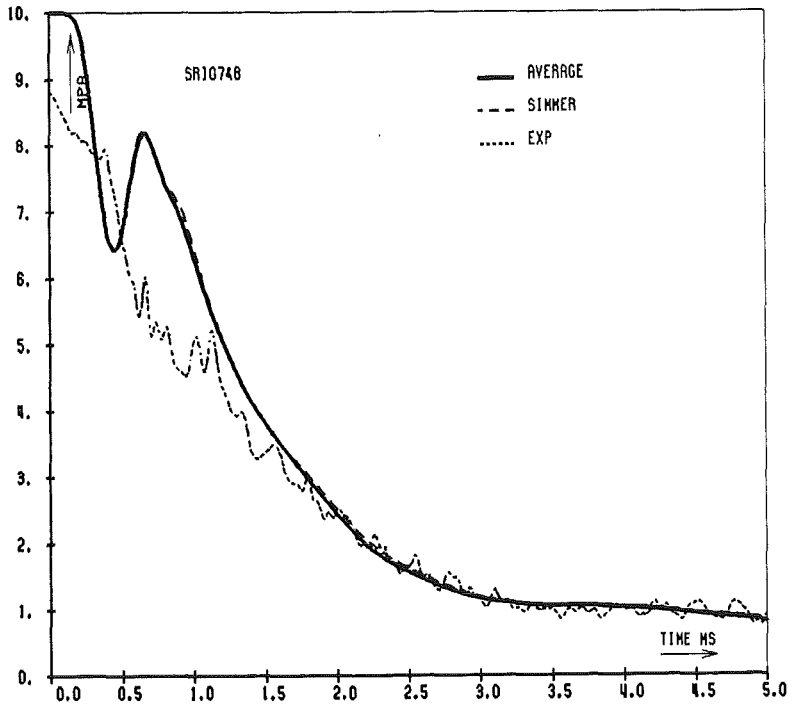

Fig. 16. Pressure at position P1

3.3 Kinetic energy

As stated in /5/ it is difficult to estimate the uncertainties in the experimental values of the kinetic energy. The uncertainty in the displaced volumes caused an error of about $\pm$ 40% in the kinetic energy. In Fig. 17-20 the kinetic energy is shown as a function of time. For the experiments 5&6 the computational results lie in the uncertainty range of the experimental values of the kinetic energy. For the later time the development of the kinetic energy is different for all approximation schemes, because the pressure loss coefficient ζ depends on the approximation scheme (section 5.1). The coarse non-uniform subgrid influences also the coefficient ζ. ζ is lowered because the kinetic energy is increased (Fig. 19).

In the case of experiments 7&8 the calculated kinetic energies deviate more from the experimental values than predicted by the estimated error of 40%. The reason for the overprediction could be that the vorticity cannot be modeled in SIMMER-II.

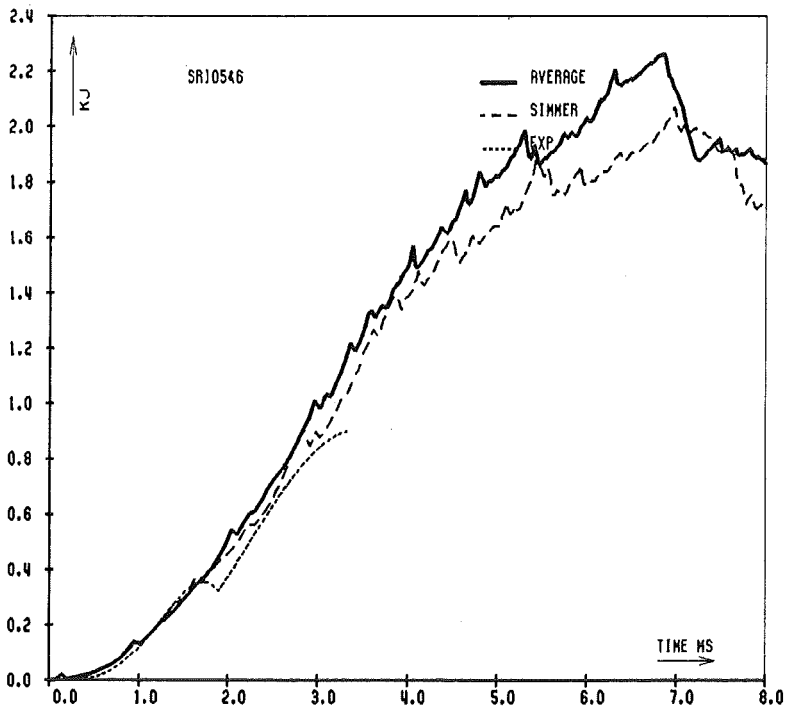

Fig. 17. Kinetic energy of the liquid

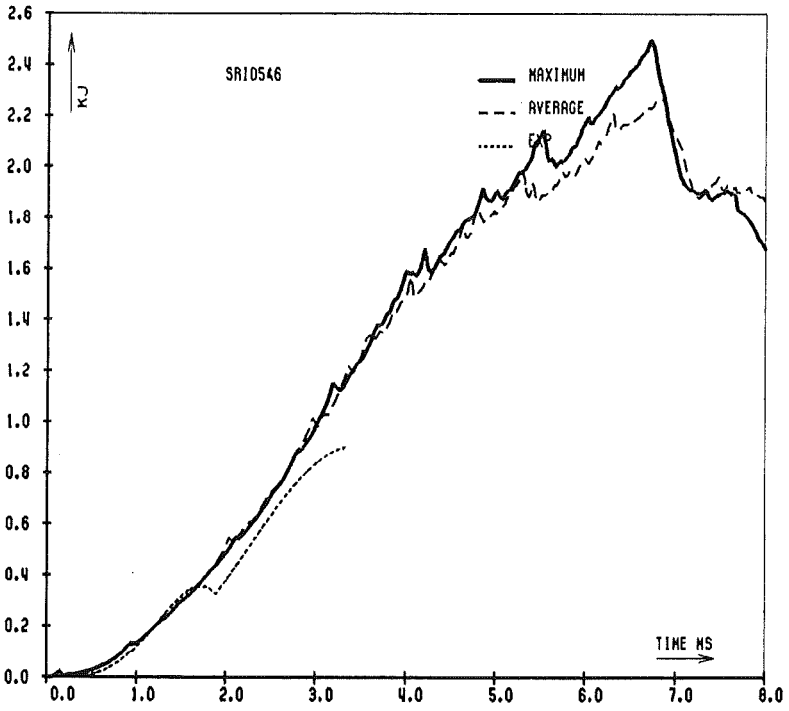

Fig. 18. Kinetic energy of the liquid

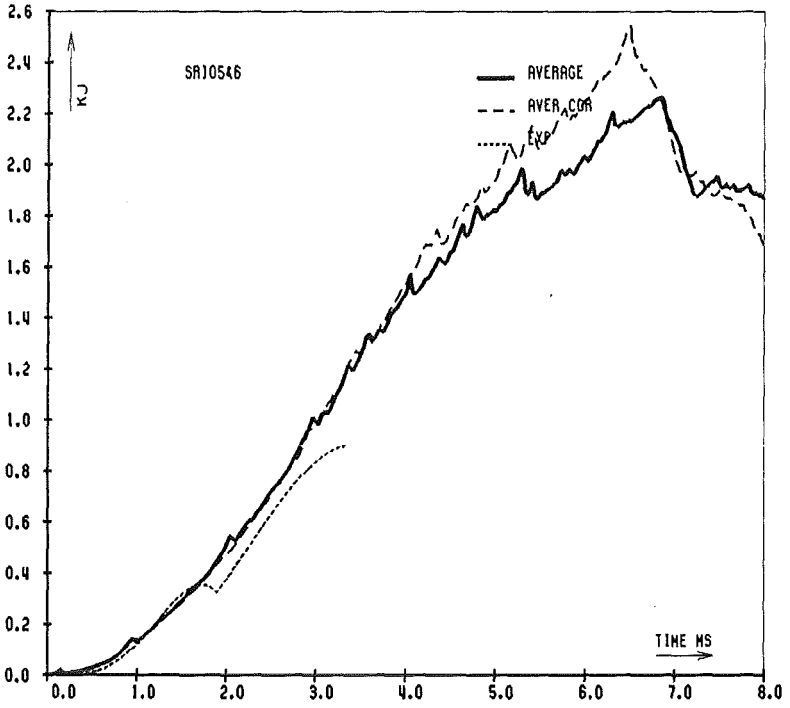

Fig. 19. Kinetic energy of the liquid

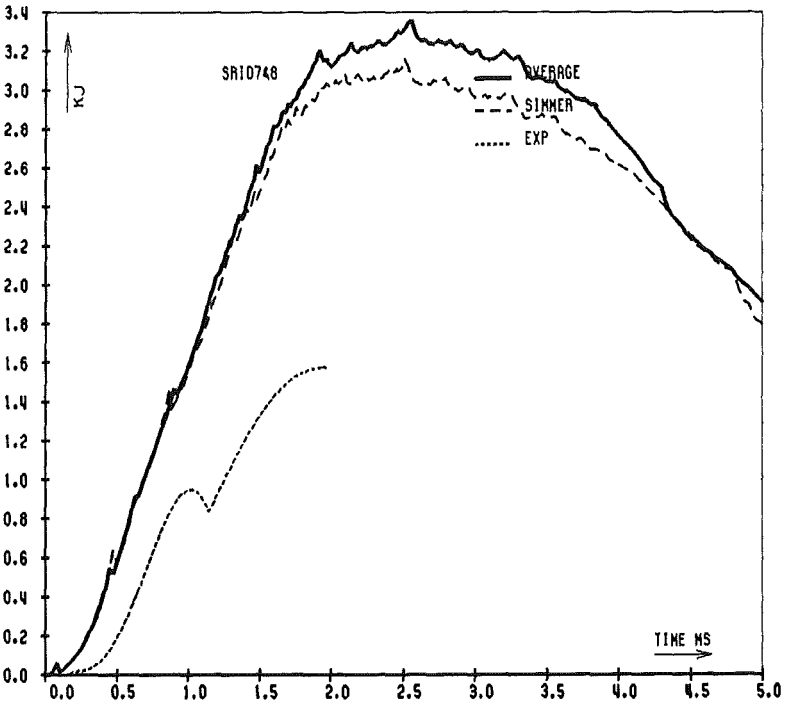

Fig. 20. Kinetic energy of the liquid

3.4 Displaced volumes

The displaced volumes in the experiments are derived from the digitized movement of the neutral density beads with an accuracy of about $\pm$ 10%. The volume calculated from the SIMMER-II results are based on the gas volume of the expanding bubble. The displaced volumes are compared with each other in Fig. 21-22. The computational results underpredict the displaced volumes in the case of experiments 5&6 and overpredict the 7&8 experimental data.

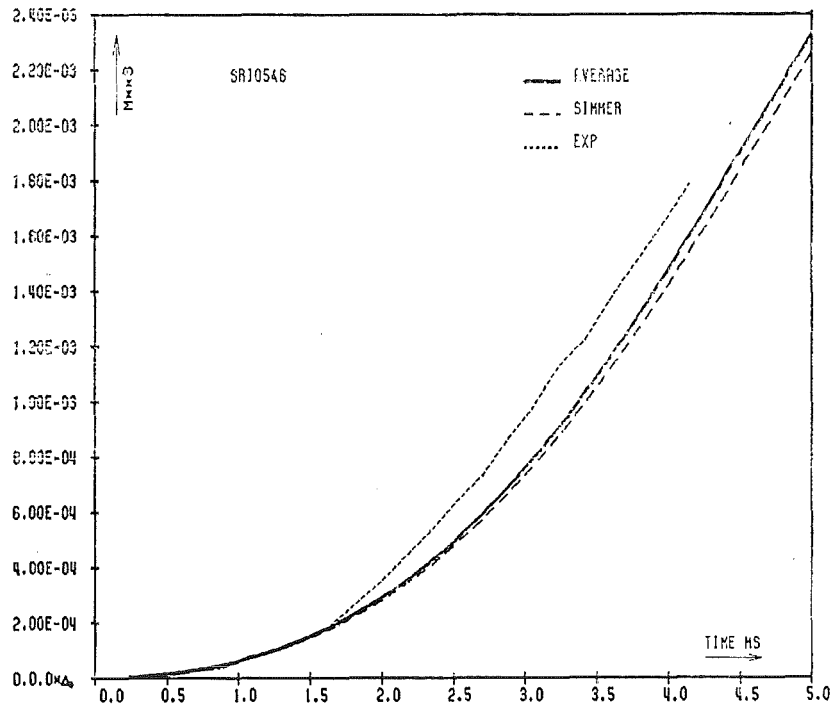

Fig. 21. Displaced water volume

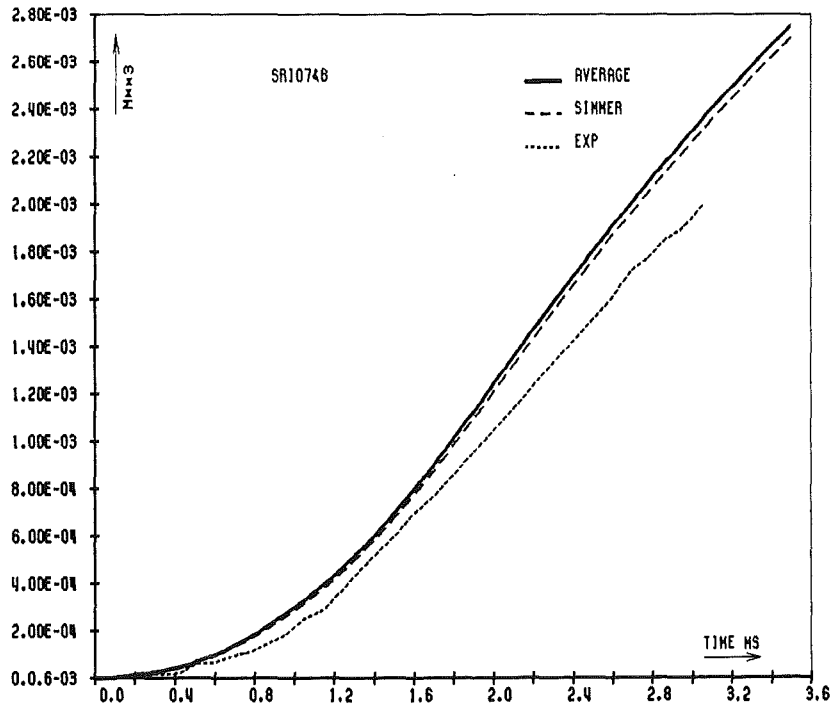

Fig. 22. Displaced water volume

Conclusion

The approximation of the volume fraction in the pressure gradient term used in the original SIMMER-II code leads to unacceptable results for the pressure change in the presence of a sudden expansion for a wide range of area ratios. This error is responsible for too low mass flow rates through an area change in SIMMER-II calculations. The proposed approximations of the pressure gradient term based on theoretical considerations remove these difficulties and give a satisfactory pressure rise in a sudden expansion. Therefore they have been implemented in the SIMMER-II code.

The pressure drop predicted from the SIMMER-II momentum equation is too high in comparison with the experimental data in the case of a sudden contraction. The pressure difference calculated for the proposed approximation schemes are in a better agreement with experiment than the results of the original SIMMER-II code.

The SNR-300 type expansion phase experiments with a dipplate are used to examine the proposed approximation schemes. The porosity of the dipplate is not increased as it was the case in former SIMMER-II calculations. The results obtained with the proposed approximation schemes are comparable with the SIMMER-II results if the porosity of the plate is increased artificially to about 0.4. Especially, the integral quantities show a satisfactory agreement with the experiments with the 2.15 MPa source. In the experiments with the high pressure source the kinetic energy is overestimated considerably, whereas the amplitude of the impact pressure is strongly underestimated and smeared out over a wide time region. Generally, the SIMMER-II solution algorithm causes difficulties in representing local quantities like pressure values.

Acknowledgement

The author is deeply indebted to K. Küfner for numerous helpful discussions and for providing detailed information about previous analyses with the SIMMER-II code.

Appendix

SIMMER-II 10 Input Data Set for the SNR05 & SNR06 Experiments

```
     0      0      0      0
     4      0      0      0      0      1      2      1  5000      0
        ----------------------------------------------------
 ------                                                        ------
 ------  SRI SIMULATION EXPERIMENTS  --->  S N R 0 5           ------
 ------                                                        ------
      0.0080          -1.         0.98
    19     51
 *****************  FLUID DYNAMICS INTEGER INPUT *********************************
    12     51      0      0      5      0      6      0     13                   31
     0      0      0      0      0      0      0      0      0      0
     1      1      0      0      0      0      0      0      0      0
     1      1
     6    100    500     50     20      5      1     -1      2      6      6      1
******************  PROBLEM DIMENSIONS AND OPERATIONAL CONTROLS *************
  0.00900000            5   0.0084670            8   0.0083000           11
  0.00990000           13   0.0050000           14   0.0102000           16
  0.00820000           19
  0.05090400            1   0.0509040            2   0.0509040            5
  0.02302800           10   0.0129000           13   0.0108500           15
  0.00984200           27   0.0054750           28   0.0031750           33
  0.00317500           37   0.005100            38   0.0091650           48
  0.0075000            51
         0.5          0.0         -9.8        1.E-4
      0.0001      1.0E-06       0.0001        0.001
      1.E-12       1.E-12       1.E-12       1.0E-5          1.0
        0.02         0.90          0.5        100.0         100.0         100.0
*******  EDIT CONTROLS AND POSTPROCESSOR CONTROLS  ****************************
 0.0
      0.0050       0.0050
 0.0
      0.0500       4.0000
 0.0
      2.5E-6       2.5E-6
 0.0
      1.0E-9       1.0E-9
 0.0
      1.0E-1

      1.0E05
0.0
     1.0E+30      1.0E+30      1.0E+30      1.0E+30      1.0E+30      1.0E+30
     1.0E+30      1.0E+30      1.0E+30      1.0E+30      1.0E+30      1.0E+30
     1.0E+30      1.0E+30      1.0E+30
     1.0E+30      1.0E+30      1.0E+30      1.0E+30      1.0E+30      1.0E+30
     1.0E+30      1.0E+30      1.0E+30      1.0E+30      1.0E+30      1.0E+30
     1.0E+30      1.0E+30      1.0E+30      1.0E+30      1.0E+30      1.0E+30
     1.0E+30      1.0E+30      1.0E+30      1.0E+30      1.0E+30      1.0E+30
 *****************  VIEW POINT PARAMETERS  ***************************************

 *****************  TIME STEP CONTROLS *******************************************
 0.0000       1.00000E-06 1.00000E-09         0.25
     2.5E-05  0.50          10.0        1.0          1.0          1.0
 1.0          0.0          0.0          0.0          0.0                 1.E-10
```

```
**********  STRUCTURE AND SOLID FAILURE PARAMETERS **********
        0.          0.          0.          0.          0.
        0.
        1.          1.          1.          1.          1.
     3.E+6       1.E+6       7.E+5       8.E+5       9.E+5       2.E+3
     3.E+4       9.E+3       2.E+1

********** FUEL PROPERTIES AND EQUATION OF STATE **********
9890.0      638.0       3100.0      2.76000E+05 2.0
8580.0      504.0       0.45        2.5         4.30000E-03
1.44000E+11 5.17080E+04 0.0         2.62000E+06 8400.0      0.597
511.0       1.05                4.4 0.00000E+08 270.0       6468.
     0.0            0.0

********** STEEL PROPERTIES AND EQUATION OF STATE **********
7365.0      639.0       1700.0      2.60000E+05 25.0
6100.0      750.0       1.6         20.0        5.36000E-03
1.33800E+11 4.33700E+04 0.0         8.17000E+06 10000.0     0.360
492.0       1.26                1.64 0.00000E+09 56.0       7700.
     0.0            0.0

WATER PROPERTIES AND EQUATION OF STATE
      1000.     2090.00      273.16    3.334E+5         .68
    1001.78      4217.1      0.0727         .68      1.0E-4
3.17771E+10 4.70579E+03         0.0 3.22689E+06     647.286    0.390597
      1402.       1.329       3.737  2.93390E+6         18.         32.
    316.957       95.77

********** CONTROL MATERIAL PROPERTIES AND EQUATION OF STATE *****
2520.0      1893.0      2623.0      2.50000E+05 83.74
2520.0      1890.0      1.0         80.0        1.00000E-03
4.28600E+14 8.36800E+04 0.0         5.00000E+06 7107.0      0.350
500.0       1.50                1.46 0.00000E+09 55.3       5472.
     0.0            0.0
*** FISSION (NITROGENE N2!) GAS PROPERTIES AND EQUATION OF STATE *****
0.0
0.0
1.00000E+11 4.00000E+04 0.0         5.00000E+06     126.2   0.3
     727.0    1.404          3.798       0.00      28.013         71.4
     0.0            0.0
**********  COMPONENT PROPERTIES **************************************
9890.0      9890.0      9890.0      9890.0      7365.0      7365.0
2520.0      0.0
8580.0      8580.0      6100.0     1000.00      2520.0      9890.0
9890.0      7365.0      0.0
2.00000E+03 2.00000E+03 2.00000E+03 1.50000E+03 2.00000E+03 2.00000E+03
2.00000E+03 2.00000E+03 2.00000E+03
**********  HEAT TRANSFER CORRELATION DATA **********
        0.0         0.0         0.0         0.0         0.0         0.0
        0.0         0.0         0.0         0.0         0.0         0.0
        0.0         0.0         0.0
      0.023         0.8         0.4         0.0
      0.025         0.8         0.8         5.0
```

```
      1.0E-10          0.8          0.4          0.0
        0.023          0.8          0.4          0.0
      1.0E-10          0.8          0.4          0.0
      1.0E-10          0.8          0.4          0.0
********************  DRAG CORRELATION DATA  ************************************
          1.0         22.0       2.0E-4       9.2E-7          1.0
          3.0          1.0          0.5
        0.046         -0.2        0.001        0.046         -0.2        0.001
      0.00000      0.00000      0.00000      0.00000      0.00000      0.00000
      0.00000      0.00000      0.00000      0.00000      0.00000      0.00000
      0.00000      0.00000      0.00000      0.00000      0.00000      0.00000
      0.00000
********************  PARAMETER  REGION  1  (NITROGEN SOURCE) ************
          7.           0.          1.E5           0.          0.0       0.1E-04
          0.           0.        1.0E-4           0.          0.0          0.0
      1.0E+40      1.0E+40      1.0E+40           0.          0.0       0.1E-04
        293.0      1.0E+19          0.0           0.          0.0      1.00E-03
       1.0E-5
************************  PARAMETER  REGION  2 (STRUCTURES    ) ************
          5.           0.0         1.E5           0.          0.0       0.25E-2
          0.           0.0          1.0           0.  .8700407332          0.11
      1.0E+40      1.0E+40      1.0E+40      1.79E+4 1.79000E+04       5.00E+2
  293.0            1.0E+19 1.00000E+05 2.30000E-05 1.00000E-17 1.00000E-03
       1.0E-5
********************  PARAMETER  REGION  3 (COVER GAS   ) *****************
          7.           0.          1.E5           0.          0.0       0.1E-04
          0.           0.        1.0E-4           0.          0.0          0.0
      1.0E+40      1.0E+40      1.0E+40           0.          0.0       0.1E-04
        293.0      1.0E+19          0.0           0.          0.0      1.00E-03
       1.0E-5
*****  PARAMETER  REGION  4 (WATER REGION) ***************
          7.           0.          1.E5           0.          0.0       0.1E-04
          0.          0.0        1.0E-4           0.          0.0          0.0
      1.0E+40      1.0E+40      1.0E+40           0.          0.0       0.1E-04
        293.0      1.0E+19          0.0           0.          0.0      1.00E-03
       1.0E-5
*********  PARAMETER  REGION  5 ( SLIDING DOORS )      ******************
          7.           0.          1.E5           0.          0.0       0.1E-04
          0.           0.        1.0E-4           0.          0.0          0.0
      1.0E+40      1.0E+40      1.0E+40           0.          0.0       0.1E-04
        293.0      1.0E+19          0.0           0.          0.0      1.00E-03
       1.0E-5
****  PARAMETER  REGION 6 (PERFORATED DIPPLATE-20% OPEN)  *****
          5.           0.0         1.E5           0.          0.0       0.25E-2
          0.           0.0          1.0           0.  .5915818000 0.08839103
      1.0E+40      1.0E+40      1.0E+40      1.79E+4 1.79000E+04       5.00E+2
  293.0            1.0E+19 1.00000E+05 2.30000E-05 1.00000E-17 1.00000E-03
       1.0E-5
****************** VAPOR AND LIQUID VELOCITIES ON THE BOTTOM BOUNDARY ******
```

```
******* MESH CELL SET 1 : WATER REGION   ************************
     1    51     1    19     3     1     0     0     4
          0.0          0.0          0.0          0.0          0.0          0.0
          0.0          0.0          0.0
        293.0        293.0        293.0        293.0        293.0        293.0
          0.0          0.0          0.0     1019.387          0.0          0.0
          0.0          0.0
        293.0        293.0        293.0        293.0        293.0        293.0
          0.0          0.0          0.0     0.739926          0.0          0.0
        293.0
          0.0          0.0          0.0          0.0     0.000005      0.00005
******* MESH CELL SET 2 : PRESSURE SOURCE I  ********************************
     1     5     1    13     3     1     0     0     1
          0.0          0.0          0.0          0.0          0.0          0.0
          0.0          0.0          0.0
        293.0        293.0        293.0        293.0        293.0        293.0
          0.0          0.0          0.0       0.0993          0.0          0.0
          0.0          0.0
        293.0        293.0        293.0        293.0        293.0        293.0
          0.0          0.0          0.0   7.86761E-4          0.0      24.8674
        293.0
          0.0          0.0          0.0          0.0     0.000005      0.00005
******* MESH CELL SET 3 : RIGID STRUCTURE I  ******************************
     1     5    14    19     1     1     0     0     2
          0.0          0.0          0.0          0.0     6407.55       810.15
          0.0          0.0          0.0
        293.0        293.0        293.0        293.0        293.0        293.0
          0.0          0.0          0.0         10.0          0.0          0.0
          0.0          0.0
        293.0        293.0        293.0        293.0        293.0        293.0
          0.0          0.0          0.0     0.739926          0.0          0.0
        293.0
          0.0          0.0          0.0          0.0     0.000005      0.00005
******* MESH CELL SET 4 : PRESSURE SOURCE II *********************************
     6    10     1     5     3     1     0     0     1
          0.0          0.0          0.0          0.0          0.0          0.0
          0.0          0.0          0.0
        293.0        293.0        293.0        293.0        293.0        293.0
          0.0          0.0          0.0       0.0993          0.0          0.0
          0.0          0.0
        293.0        293.0        293.0        293.0        293.0        293.0
          0.0          0.0          0.0   7.86761E-4          0.0      24.8674
        293.0
          0.0          0.0          0.0          0.0     0.000005      0.00005
******* MESH CELL SET 5 : RIGID STRUCTURE II ******************************
     6    13     6    19     1     1     0     0     2
          0.0          0.0          0.0          0.0     6407.55       810.15
          0.0          0.0          0.0
        293.0        293.0        293.0        293.0        293.0        293.0
          0.0          0.0          0.0         10.0          0.0          0.0
          0.0          0.0
        293.0        293.0        293.0        293.0        293.0        293.0
          0.0          0.0          0.0     0.739926          0.0          0.0
        293.0
          0.0          0.0          0.0          0.0     0.000005      0.00005
******* MESH CELL SET  6 : SLIDING DOORS      **********************
    11    11     1     5     1     1     0     0     5
```

```
          0.0          0.0          0.0          0.0          0.0          0.0
          0.0          0.0          0.0
        293.0        293.0        293.0        293.0        293.0        293.0
          0.0          0.0          0.0       0.0993          0.0          0.0
          0.0          0.0
        293.0        293.0        293.0        293.0        293.0        293.0
          0.0          0.0          0.0  7.86761E-4          0.0     1.160795
        293.0
          0.0          0.0          0.0          0.0     0.000005      0.00005
******* MESH CELL SET 7: REFLECTOR REGION    ******************************
    14    15     6     8     1     1     0     0     2
          0.0          0.0          0.0          0.0      6407.55       810.15
          0.0          0.0          0.0
        293.0        293.0        293.0        293.0        293.0        293.0
          0.0          0.0          0.0         10.0          0.0          0.0
          0.0          0.0
        293.0        293.0        293.0        293.0        293.0        293.0
          0.0          0.0          0.0     0.739926          0.0          0.0
        293.0
          0.0          0.0          0.0          0.0     0.000005      0.00005
******* MESH CELL SET 8 : SHIELDING TANK        ******************************
    14    27    14    16     1     1     0     0     2
          0.0          0.0          0.0          0.0      6407.55       810.15
          0.0          0.0          0.0
        293.0        293.0        293.0        293.0        293.0        293.0
          0.0          0.0          0.0         10.0          0.0          0.0
          0.0          0.0
        293.0        293.0        293.0        293.0        293.0        293.0
          0.0          0.0          0.0     0.739926          0.0          0.0
        293.0
          0.0          0.0          0.0          0.0     0.000005      0.00005
******* MESH CELL SET  9 : COVER GAS VOLUME    ************************
    39    51     1    19     1     1     0     0     3
          0.0          0.0          0.0          0.0          0.0          0.0
          0.0          0.0          0.0
        293.0        293.0        293.0        293.0        293.0        293.0
          0.0          0.0          0.0       0.0993          0.0          0.0
          0.0          0.0
        293.0        293.0        293.0        293.0        293.0        293.0
          0.0          0.0          0.0  7.86761E-4          0.0     1.160795
        293.0
          0.0          0.0          0.0          0.0     0.000005      0.00005
******* MESH CELL SET 10: DIPPLATE SUPPORT      ******************************
    32    48    12    14     1     1     0     0     2
          0.0          0.0          0.0          0.0      6407.55       810.15
          0.0          0.0          0.0
        293.0        293.0        293.0        293.0        293.0        293.0
          0.0          0.0          0.0         10.0          0.0          0.0
          0.0          0.0
        293.0        293.0        293.0        293.0        293.0        293.0
          0.0          0.0          0.0     0.739926          0.0          0.0
        293.0
          0.0          0.0          0.0          0.0     0.000005      0.00005
******* MESH CELL SET 11 : GAP ABOVE SUPPORT     ************************
    49    51    12    14     1     1     0     0     3
          0.0          0.0          0.0          0.0          0.0          0.0
          0.0          0.0          0.0
```

```
        293.0          293.0          293.0          293.0          293.0          293.0
          0.0            0.0            0.0         0.0993            0.0            0.0
          0.0            0.0
        293.0          293.0          293.0          293.0          293.0          293.0
          0.0            0.0            0.0   7.86761E-4            0.0        1.160795
        293.0
          0.0            0.0            0.0            0.0       0.000005        0.00005
***** MESH CELL SET 12 -  DIPPLATE
    32     33      1     11      3      1      1      0      6
          0.0            0.0            0.0            0.0         4357.0         651.00

                                     293.           293.
                                                 319.60000

                                     293.
          0.0            0.0            0.0   7.86761E-4            0.0        1.160795
        293.
  0.0           0.0            0.0            0.0          0.0001         0.001
```

References

/1/ W.H. Archer, Trans. ASCE 76 (1913), 999-1026

/2/ S. Whitaker, Introduction to Fluid Mechanics, Englewood Cliffs: Prentice-Hall (1968)

/3/ H.W. King, E.F. Brater, Handbook of Hydraulics, New York: McGraw-Hill Book Company (1963)

/4/ L.L. Smith et al., SIMMER-II: A Computer Program for LMFBR Disrupted Core Analyses, NUREG/CR-0453, LA-7515.M, Rev. (June 1980)

/5/ K. Küfner, P. Schmuck, R. Fröhlich, SIMMER-II Analyses of Expansion Phase Experiments in SNR Geometry, Report KfK 3633 (1984)

/6/ Robert J. Tobin: unpublished research report (1981)

/7/ I.E. Idelchik: Handbook of Hydraulic Resistance, Berlin: Springer Verlag (1986)